Grid Orientation Effect and MultiPoint Flux Approximation

Robert Eymard, Cindy Guichard and Roland Masson

Abstract Some cases of nonlinear coupling between a diffusion equation, related to the computation of a pressure field within a porous medium, and a convection equation, related to the conservation of a species, lead to the apparition of the so-called grid orientation effect. We propose in this paper a new procedure to eliminate this Grid Orientation Effect, only based on the modification of the stencil of the discrete version of the convection equation. Numerical results show the efficiency and the accuracy of the method.

Key words: Grid Orientation Effect, Two Phase Porous Media Flow, Finite Volume Methods
MSC2010: 76S05, 65M08, 76E06

1 Introduction

In the 1980's, numerous papers have been concerned with the so-called grid orientation effect, in the framework of oil reservoir simulation. This effect is due to the anisotropy of the numerical diffusion induced by the upstream weighting scheme, and the computation of a pressure field, solution to an elliptic equation in which the diffusion coefficient depends on the value of the convected unknown. This problem has been partly solved in the framework of industrial codes, in which the meshes are structured and regular (mainly based on squares and cubes). The literature on this problem is huge, and is impossible to exhaustively quote; let us only cite [3, 4, 6, 10, 11] and references therein. In the 2000's, a series of new schemes have been introduced in order to compute these coupled problems on general grids

R. Eymard
Université Paris-Est, France, e-mail: robert.eymard@univ-mlv.fr

C. Guichard (work supported by ANR VFSitCom)
Université Paris-Est and IFP Energies nouvelles, France, e-mail: cindy.guichard@ifpen.fr

R. Masson
IFP Energies nouvelles, France, e-mail: roland.masson@ifpen.fr

[1, 2, 5, 8]. But, in most of the cases, the non regular meshes conserve structured directions, although the shape of the control volumes is no longer that of a regular cube. This is the case for the Corner Point Geometries [9] widely used in industrial reservoir simulations. The control volumes which are commonly used in 3D reservoir simulations are generalised "hexahedra", in the sense that each of them is neighboured by 6 other control volumes. In this case, the stencil for the pressure resolution may have a 27-point stencil (using for instance a MPFA scheme). Nevertheless, selecting a 27-point stencil instead of a 7-point stencil for the pressure resolution has no influence on the Grid Orientation Effect, which results from the stencil used in upstream weighted mass exchanges coupled with the pressure resolution.

In order to overcome this problem, we study here a generalisation of methods consisting in increasing the stencil of the convection equation, without modifying the pressure equation. The method will be presented on a simplified problem, modelling immiscible two-phase flow within a porous medium. Let $\Omega \subset \mathbb{R}^d$ (with $d = 2$ or 3) be the considered space domain. We consider the following two-phase flow problem in Ω:

$$\begin{cases} u_t - \mathrm{div}(k_1(u)\Lambda\nabla p) = 0 \\ (1-u)_t - \mathrm{div}(k_2(u)\Lambda\nabla p) = 0, \end{cases} \tag{1}$$

where $u(x,t) \in [0,1]$ is the saturation of phase 1 (for example water), and therefore $1-u(x,t)$ is the saturation of phase 2, k_1 is the mobility of phase 1 (increasing function such that $k_1(0) = 0$), k_2 is the mobility of phase 2 (decreasing function such that $k_2(1) = 0$), and p is the common pressure of both phases (the capillary pressure is assumed to be negligible in front of the pressure gradients due to injection and production wells) and we consider a horizontal medium with permeability tensor Λ. It is therefore possible to see System (1) as the coupling of an elliptic problem with unknown p and a nonlinear scalar hyperbolic problem with unknown u:

$$\begin{cases} m(u) = k_1(u) + k_2(u), f(u) = \dfrac{k_1(u)}{m(u)} \\ \mathrm{div}F = 0 \text{ with } F = -m(u)\Lambda\nabla p \\ u_t + \mathrm{div}(f(u)F) = 0 \end{cases} \tag{2}$$

We then consider a MultiPoint Flux Approximation finite volume scheme for the approximation of Problem (1), coupled with an upstream weighting scheme for the mass exchanges. Such a scheme may be written :

$$F_{K,L}^{(n)} = m_{KL}^{(n)} \sum_{M \in \mathscr{M}} a_{KL}^M p_M^{(n+1)} \text{ with } \sum_{M \in \mathscr{M}} a_{KL}^M = 0 \tag{3}$$

$$\sum_{L \in \mathscr{N}_K} F_{K,L}^{(n)} = 0 \tag{4}$$

$$F_{K,L}^{(n)} + F_{L,K}^{(n)} = 0 \tag{5}$$

$$|K| \left(u_K^{(n+1)} - u_K^{(n)} \right) + \delta t^n \sum_{L \in \mathscr{N}_K} \left(f(u_K^{(n)})(F_{K,L}^{(n)})^+ - f(u_L^{(n)})(F_{K,L}^{(n)})^- \right) = 0. \tag{6}$$

In the above system, we denote by $\mathscr{M}$ the finite volume mesh of Ω, K,L are control volumes, $\mathscr{N}_K$ is the set of the neighbours of K (*i.e.* control volumes exchanging fluid mass with K), n is the time index and δt^n is the time step ($\delta t^n = t^{(n+1)} - t^{(n)}$), $p_M^{(n)}$ and $u_M^{(n)}$ are respectively the pressure and the saturation in control volume M at time $t^{(n)}$. The coefficients a_{KL}^M are computed with respect to the geometry of the mesh and to Λ. The value $m_{KL}^{(n)}$ is any average value (arithmetic or harmonic) of the values $m(u_K^{(n)})$ and $m(u_L^{(n)})$. Then $F_{K,L}^{(n)}$ is the approximation of $F \cdot \boldsymbol{n}$ at the interface $K|L$ between control volumes K and L at time step n, and, for all real a, the values a^+ and a^- are respectively defined by $\max(a,0)$ and $\max(-a,0)$.

The set $\mathscr{N}_K$ of the neighbours of K is classically defined as all the control volumes which have a common face with K. But, as we show in this paper, this notion may be relaxed. Defining the notion of "stencil" $S \subset \mathscr{M}^2$ by $S = \{(K,L) \in \mathscr{M}^2, L \in \mathscr{N}_K\}$, this stencil is then equal to the set of all $(K,L) \in \mathscr{M}^2$ such that $F_{K,L}^{(n)}$ may be different from 0. In view of (5), S must verify the symmetry property

$$S \subset \mathscr{M}^2 \text{ and } \forall (K,L) \in S, (L,K) \in S. \tag{7}$$

As we stated in the introduction, the drawback of the use of this stencil for practical problems, where $F_{K,L}^{(n)}$ is computed from the resolution of a pressure equation, is that it leads to the Grid Orientation Effect. Therefore, we want to replace (6) by

$$|K| \left(u_K^{(n+1)} - u_K^{(n)} \right) + \delta t^n \sum_{L \in \widehat{\mathscr{N}_K}} \left(f(u_K^{(n)}) (\widehat{F}_{K,L}^{(n)})^+ - f(u_L^{(n)}) (\widehat{F}_{K,L}^{(n)})^- \right) = 0, \tag{8}$$

where the new stencil $\widehat{S}$, defined by $\widehat{S} = \{(K,L) \in \mathscr{M}^2, L \in \widehat{\mathscr{N}_K}\}$, is such that the Grid Orientation Effect is suppressed. In (8), the values of the fluxes $(\widehat{F}_{K,L}^{(n)})_{(K,L) \in \widehat{S}}$ will be set such that the two following properties hold: the flux continuity holds

$$\widehat{F}_{K,L}^{(n)} + \widehat{F}_{L,K}^{(n)} = 0, \ \forall (K,L) \in \widehat{S}, \tag{9}$$

and the balance in the control volumes is the same as that satisfied by the fluxes $(F_{K,L}^{(n)})_{(K,L) \in S}$:

$$\sum_{L, (K,L) \in \widehat{S}} \widehat{F}_{K,L}^{(n)} = \sum_{L, (K,L) \in S} F_{K,L}^{(n)}, \ \forall K \in \mathscr{M}. \tag{10}$$

In view of (15), we again prescribe the symmetry property

$$\widehat{S} \subset \mathscr{M}^2 \text{ and } \forall (K,L) \in \widehat{S}, \ (L,K) \in \widehat{S}. \tag{11}$$

The section 2 of this paper is devoted to the description of a method for constructing $\widehat{F}_{K,L}^{(n)}$ for a given stencil $\widehat{S}$, which ensures properties (9) and (10) (corresponding, for a given n, to (15) and (16) below). The application of this method to the case of an initial five-point pattern stencil S and of a nine-point stencil $\widehat{S}$ is detailed in Section 3.

Then numerical tests show the efficiency of the method to fight the Grid Orientation Effect (section 4).

2 Construction of $\widehat{F}_{K,L}$ in the new stencil $\widehat{S}$

The method presented in this section concerns the reconstruction of the fluxes, which has to be applied to each time step. Hence, for the simplicity of notation, we drop the index n in this section. For a stencil $\widehat{S} \subset \mathscr{M}^2$ such that (11) holds and for given $(K,L) \in \mathscr{M}^2$, the set $\widehat{\mathscr{S}_{K,L}}$ of the paths from K to L following $\widehat{S}$ is defined by

$$\widehat{\mathscr{S}_{K,L}} := \left\{ P = \left\{ \begin{array}{l} (K_i,K_{i+1}), i = 1,\dots,N-1 \text{ with } K_1 = K,\ K_N = L \\ \text{and } K_i \neq K_j \text{ for } i \neq j = 1,\cdots,N \end{array} \right\} \subset \widehat{S} \right\}. \quad (12)$$

We denote by $\sharp\widehat{\mathscr{S}_{K,L}}$ the cardinality of $\widehat{\mathscr{S}_{K,L}}$, i.e. the number of paths P from K to L following $\widehat{S}$. For any $P = \{(K_i,K_{i+1}), i = 1,\dots,N-1\} \in \widehat{\mathscr{S}_{K,L}}$, we denote by $P^{\leftarrow}$ the inverse path from L to K following $\widehat{S}$, defined by $P^{\leftarrow} = \{(K_{i+1},K_i), i = 1,\dots,N-1\}$.

We may now state the following result.

Lemma 1 (New stencil and fluxes). *Let $\mathscr{M}$ be a finite set, let $S \subset \mathscr{M}^2$ be given such that* (7) *holds. Let $(F_{K,L})_{(K,L)\in S}$ be a family such that the property*

$$F_{K,L} + F_{L,K} = 0,\ \ \forall (K,L) \in \mathscr{M}^2$$

holds. Let $\widehat{S} \subset \mathscr{M}^2$ be given such that (11) *holds and such that*

$$\forall (K,L) \in S,\ \ \sharp\widehat{\mathscr{S}_{K,L}} > 0.$$

For all $(K,L) \in S$, let $(F^P_{K,L})_{P\in\widehat{\mathscr{S}_{K,L}}}$ be a family such that

$$\forall (K,L) \in S,\ \ \textstyle\sum_{P\in\widehat{\mathscr{S}_{K,L}}} F^P_{K,L} = F_{K,L},$$

satisfying the property

$$\forall (K,L) \in S,\ \forall P \in \widehat{\mathscr{S}_{K,L}},\ F^P_{K,L} + F^{P^{\leftarrow}}_{L,K} = 0. \quad (13)$$

Then the family $(\widehat{F}_{K,L})_{(K,L)\in\widehat{S}}$, defined by

$$\forall (I,J) \in \widehat{S},\ \widehat{F}_{I,J} = \sum_{(K,L)\in S} \sum_{P\in\widehat{\mathscr{S}_{K,L}}} \xi_{I,J,P} F^P_{K,L}, \quad (14)$$

where $\xi_{I,J,P}$ is such that $\xi_{I,J,P} = 1$ if $(I,J) \in P$ and $\xi_{I,J,P} = 0$ otherwise, satisfies

$$\widehat{F}_{K,L} + \widehat{F}_{L,K} = 0,\ \forall (K,L) \in \widehat{S}, \quad (15)$$

and

$$\sum_{L,(K,L)\in\widehat{S}} \widehat{F}_{K,L} \ = \sum_{L,(K,L)\in S} F_{K,L},\ \forall K \in \mathscr{M}. \quad (16)$$

Proof. Firstly, using definitions, for a given $(I,J) \in \widehat{S}$, we have $(J,I) \in \widehat{S}$ and $\widehat{F}_{J,I} = \sum_{(L,K)\in S} \sum_{P\in\widehat{\mathscr{T}}_{L,K}} \xi_{J,I,P} F^P_{L,K}$. Then, thanks to the following equivalences

$$\begin{cases} (L,K) \in S \iff (K,L) \in S \\ P \in \widehat{\mathscr{T}}_{L,K} \iff P^{\leftarrow} \in \widehat{\mathscr{T}}_{K,L} \\ (J,I) \in P \iff (I,J) \in P^{\leftarrow}, \end{cases}$$

and using (13), we can rewrite $\widehat{F}_{J,I}$ as follows

$$\widehat{F}_{J,I} = -\sum_{(K,L)\in S} \sum_{P\in\widehat{\mathscr{T}}_{K,L}} \xi_{I,J,P} F^P_{K,L} = -\widehat{F}_{I,J},$$

which proves (15).

Secondly, for a given $I \in \mathscr{M}$, by reordering the sums, we can write that

$$\sum_{J,(I,J)\in\widehat{S}} \widehat{F}_{I,J} = \sum_{J,(I,J)\in\widehat{S}} \sum_{(K,L)\in S} \sum_{P\in\widehat{\mathscr{T}}_{K,L}} \xi_{I,J,P} F^P_{K,L} = \sum_{(K,L)\in S} \sum_{P\in\widehat{\mathscr{T}}_{K,L}} \chi_{I,P} F^P_{K,L}$$

where $\chi_{I,P} = \sum_{J,(I,J)\in\widehat{S}} \xi_{I,J,P}$ is equal to 1 if there exists $J \in \mathscr{M}$ such that $(I,J) \in P$ (therefore $I \neq L$), and to 0 otherwise. Note that, for $(K,L) \in S$ with $K \neq I$ and for $P \in \widehat{\mathscr{T}}_{K,L}$ with $\chi_{I,P} = 1$, we have $I \neq L$, $(L,K) \in S$, $P^{\leftarrow} \in \widehat{\mathscr{T}}_{L,K}$ and $\chi_{I,P^{\leftarrow}} = 1$. So, using (13), we obtain

$$\sum_{(K,L)\in S \text{ s.t. } K\neq I} \sum_{P\in\widehat{\mathscr{T}}_{K,L}} \chi_{I,P} F^P_{K,L} = 0.$$

Therefore we can write

$$\sum_{J,(I,J)\in\widehat{S}} \widehat{F}_{I,J} = \sum_{L,(I,L)\in S} \sum_{P\in\widehat{\mathscr{T}}_{I,L}} \chi_{I,P} F^P_{I,L} = \sum_{L,(I,L)\in S} \sum_{P\in\widehat{\mathscr{T}}_{I,L}} F^P_{I,L} = \sum_{L,(I,L)\in S} F_{I,L},$$

which proves (16).

3 Application to an initial five-point stencil on a structured quadrilateral mesh

Let us assume, taking the example of a 2D situation, that the initial stencil S is a five-point stencil, defined on a regular quadrilateral mesh

$$S = \{(K,L) \in \mathscr{M}^2,\ \overline{K} \textit{ and } \overline{L} \textit{ have a common edge }\}, \tag{17}$$

and that the new stencil $\widehat{S}$ is the nine-point stencil (see the figure below), defined by

$$\widehat{S} = S \cup \{(K,L) \in \mathscr{M}^2,\ \overline{K} \textit{ and } \overline{L} \textit{ have a common point }\}. \tag{18}$$

Then we define $(F^P_{K,L})_{P\in\widehat{\mathscr{S}}_{K,L}}$, for all $P \in \widehat{\mathscr{S}}_{K,L}$ and all $(K,L) \in S$ (remark that in this case, $S \subset \widehat{S}$):

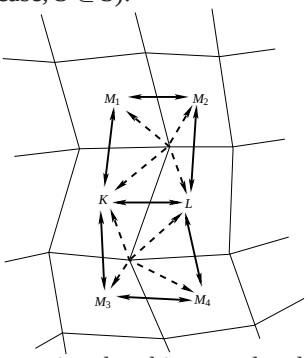

For a given $\omega > 0$ (we take the value $\omega = 0.1$ in the numerical examples), we define

$$\begin{cases} F^{P_0}_{K,L} = (1-4\omega)F_{K,L} \text{ for } P_0 = \{(K,L)\}, \\ F^{P_i}_{K,L} = \omega F_{K,L} \\ \quad \text{for } P_i = \{(K,M_i),(M_i,L)\},\ \forall i = 1,\ldots,4, \\ F^{P}_{K,L} = 0 \text{ otherwise.} \end{cases}$$

Assuming that this procedure has been applied to all initial five-point connection, let us give the resulting values of $\widehat{F}_{K,L}$ deduced from (14) in two cases:

$$\begin{cases} \widehat{F}_{K,L} = (1-4\omega)F_{K,L} \\ \widehat{F}_{K,M_2} = \omega(F_{K,L} + F_{L,M_2} + F_{K,M_1} + F_{M_1,M_2}). \end{cases}$$

4 Numerical results

The numerical tests presented here are inspired by [7]. The domain is defined by $\Omega = [-0.5,0.5]\text{x}[-0.5,0.5]\text{x}[-0.15,0.15]$. The permeability $\Lambda(\boldsymbol{x}), \boldsymbol{x} \in \Omega$ is equal to 1 if the distance from $\boldsymbol{x}$ to the vertical axis $0z$ is lower than 0.48, and to 10^{-3} otherwise (see Figure 1), which ensures the confinement of the flow in the cylinder with axis $0z$ and radius 0.48. We use two Cartesian grids, the second one deduced from the first one by a rotation of angle $\theta = \frac{\pi}{6}$ with axis Oz. The number of cells in each direction (x,y,z) are $N_x = N_y = 51$ and $N_z = 3$. At the initial state, the reservoir is assumed to be saturated by the oil phase. Water is injected at the origin by an injection well. Two production wells, denoted by P_1 and P_2, are respectively located at the points $(-0.3\cos\frac{\pi}{3}, -0.3\sin\frac{\pi}{3}, 0)$ and $(0.3\cos\frac{\pi}{3}, -0.3\sin\frac{\pi}{3}, 0)$ (that means that the three wells are numerically taken into account as source terms in the middle layer of the mesh). The oil and water properties are respectively denoted by the index o and w. The viscosity ratio between the two phases is given by $\mu_o/\mu_w = 100$ and, the density ratio is given by $\rho_o/\rho_w = 0.8$. We use Corey-type relative permeability, $k_{r_w} = S_w^4$ and $k_{r_o} = S_o^2$. We use the method described in Sections 2 and 3, with $\omega = 0.1$ for all grid blocks which are inscribed in the cylinder (this value, also used in [6], provides the less sensitive numerical results with respect to the grid orientation). The same value for the time step is used for all the computations, which are stopped once a given quantity of water has been injected. Note that, in the mesh depicted on the right part of Figure 1, the line (P_2, O) is the axis $0y$ of the mesh. We

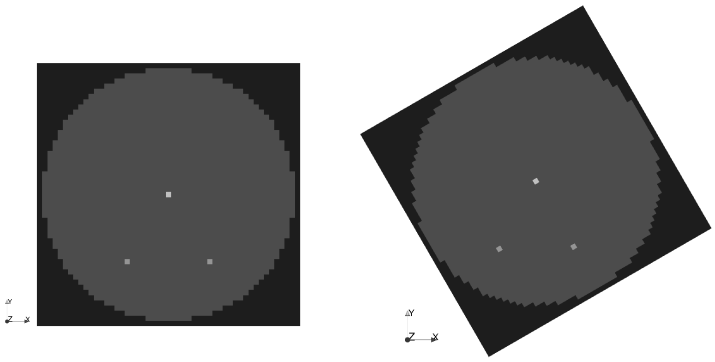

Fig. 1 The two meshes used. In grey scale, the highest permeability zone, in black the lower permeability zone. Squares indicate wells.

then see on Figure 2 the resulting contours of the saturation. We observe that the results obtained using the method described in Sections 2 and 3 look very similar in the two grids, whereas the ones obtained using the five-point stencil are strongly distorted by the Grid Orientation Effect.

5 Conclusion

The method presented in this paper is a natural extension of the nine-point schemes defined some decades ago on regular grids. Its advantage is that it applies on the structured but not regular grids used in reservoir simulation, in association with MultiPoint Flux Approximation finite volume schemes. It demands no further modification to the standard industrial codes, since the modification are only the definition of new coefficients a_{KL}^M used in (3).

References

1. Aavatsmark, I., Eigestad, G.T.: Numerical convergence of the MPFA O-method and U-method for general quadrilateral grids. Int. J. Numer. Meth. Fluids **51**, 939–961 (2006)
2. Agelas, L., Masson, R.: Convergence of the finite volume MPFA O scheme for heterogeneous anisotropic diffusion problems on general meshes. C. R. Math. **346**, 1007–1012 (2008)
3. Aziz, K., Ramesh, A.B., Woo, P.T.: Fourth SPE comparative solution project: comparison of steam injection simulators. J. Pet. Tech. **39**, 1576–1584 (1987)
4. Corre, B., Eymard, R., Quettier, L.: Applications of a thermal simulator to field cases, SPE ATCE (1984)
5. Dawson, C., Sun, S., Wheeler, M.F.: Compatible algorithms for coupled flow and transport. Comput. Meth. Appl. Mech. Eng. **193**, 2565–2580 (2004)
6. Eymard, R., Sonier, F.: Mathematical and Numerical Properties of Control-Volumel Finite-Element Scheme for Reservoir Simulation. SPE Reservoir Eng. **9**, 283–289 (1994)

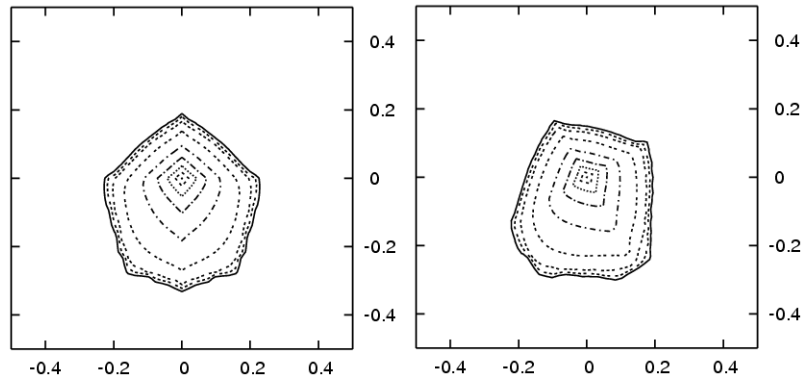

(a) $\theta = 0$, stencil S (b) $\theta = \frac{\pi}{6}$, stencil S

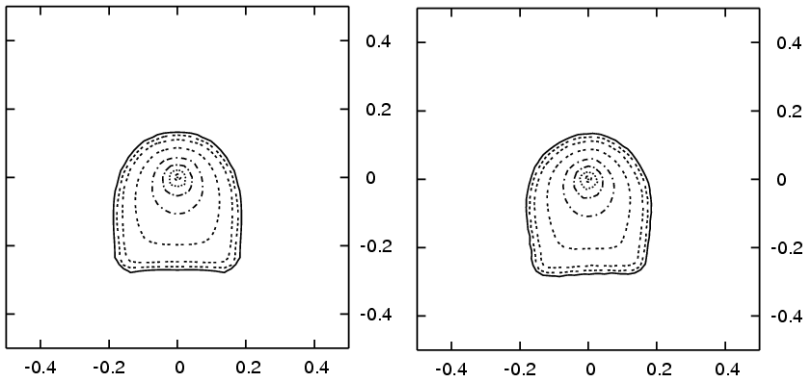

(c) $\theta = 0$, stencil $\widehat{S}$ (d) $\theta = \frac{\pi}{6}$, stencil $\widehat{S}$

Fig. 2 Water saturation contours $S_w = 0.1,\ 0.2, \ldots, 1$ at the same time.

7. Keilegavlen, E., Kozdon, J., Mallison, B.T.: Monotone Multi-dimensional Upstream Weighting on General Grids. Proceeding of ECMOR XII (2010)
8. Lipnikov, K., Moulton, J.D., Svyatskiy, D.: A multilevel multiscale mimetic (M3) method for two-phase flows in porous media. J. Comput. Phys. **14**, 6727–6753 (2008)
9. D.K. Ponting. Corner Point Geometry in reservoir simulation. *In Clarendon Press, editor*, Proc. ECMOR I, 45–65, Cambridge, 1989.
10. Vinsome, P., Au, A.: One approach to the grid orientation problem in reservoir simulation. Old SPE J. **21**, 160–161 (1981)
11. Yanosik, J.L., McCracken, T.A.: A nine-point, finite-difference reservoir simulator for realistic prediction of adverse mobility ratio displacements. Old SPE J. **19**, 253–262 (1979)

The paper is in final form and no similar paper has been or is being submitted elsewhere.